Journal of Thermal Biology 35 (2010) 441–449

Contents lists available at ScienceDirect

Journal of Thermal Biology

journal homepage: www.elsevier.com/locate/jtherbio

Environmental and physiological simulation of heat stroke: A case study analysis and validation

R.R. Gonzalez [a,*], C. Halford [b], E.M. Keach [c]

[a] Biology Department, New Mexico State University, Las Cruces, 2274 Highway 61, San Lorenzo, NM 88041, USA
[b] Center for Energy Research, University of Nevada, Las Vegas, NV 89101, USA
[c] Eckley M. Keach Law Offices, Las Vegas, NV 89101, USA

ARTICLE INFO

Article history:
Received 29 August 2010
Accepted 24 September 2010

Keywords:
Thermoregulation
Modeling
Dehydration

ABSTRACT

1. In this study, we examined by *post hoc* meta- analysis the likely physiological consequences of environmental stress in a 56-year old, mentally impaired woman who suffered heat stroke after being trapped in an abandoned car on a hot, sunny day in August in a Las Vegas, NV, parking lot. At 1400 h, she entered the car and at 1830 h, after severe exposure to heat stress inside the car, she was found unresponsive to resuscitation.

2. We completed an extensive environmental analysis (air and mean radiant temperatures, humidity) from 1400 h to 1830 h for 16 days in the interior space of an exemplar auto stationed at the University of Nevada, Las Vegas. We recorded in this vehicle the time course of heat stress by direct solar load similar to the day of the incident completed for 16 days from August 25 through September 16, 2009. We next employed a physiological model of thermoregulatory and cardiovascular responses to forecast and validate key responses to the thermal input data from the environmental analysis.

3. We validated changes that were consistent with severe imbalances in thermoregulation. Core, skin, and blood temperature increases, and severe fluid loss $>5\%$ were simulated in the analysis that reliably forecasted heat stroke (core temperature $\geq 41\ ^{\circ}C$) and, more likely than not, non-compensable brain damage.

4. We recommend the use of such consequence physiological modeling as an added adjuvant and tool, along with other emergency features, that might serve to minimize and optimize survival tactics used in curbing exertional and climatic heat stroke.

1. Introduction: review of environmental heat stress in humans

The human thermoregulatory system is intricately controlled by the preoptic/anterior hypothalamus which responds to changes in afferent thermal drives from skin and internal body temperature sensors (Boulant and Gonzalez, 1977; Boulant, 1996; Gagge and Gonzalez, 1996; Sawka et al., 1996; Kenney et al., 2004). Extensive research shows that such afferent information synapses on temperature sensitive neurons in the anterior hypothalamus where there is a high concentration of neurons that respond to appropriate thermal signals to activate either heat loss responses or heat conservation responses (Boulant, 1996). The appropriate effector response is met by changes deviating from a narrow range in anterior hypothalamic temperature either by increases in sweating and skin blood flow to eliminate excess heat or by shivering, thereby escalating metabolic response, whenever the hypothalamic set point is higher or lower than the normal range (Gagge and Gonzalez, 1996; Sawka et al., 1996). Core body temperature is maintained within a very narrow range of normality (generally between 36 and 39 °C (96.8–102.2 °F), even in extreme environmental conditions, through an intricate system integrating various physical and biochemical processes coordinated by the hypothalamus. The rate and amount of heat exchanged by the body via the skin surface is governed by fundamental laws of thermodynamics (Gagge and Gonzalez, 1996). When heat cannot be dissipated effectively, as may happen when the environmental temperature is elevated or as a result of strenuous physical exercise, heat syndromes develop (Sawka et al., 1996; Shapiro and Seidman, 1990; Wallace et al., 2005). The latter have a wide spectrum, ranging from the relatively mild heat rash to heat edema, heat cramps, heat exhaustion, exertional heat injury, and the very serious, life-threatening, often fatal, heat stroke (Kenney et al., 2004; Garigan and Ristedt, 1999; Epstein et al., 1999; Kosaka et al., 2004).

Heat exhaustion is defined by the U.S. Army as the appearance of a core (rectal) temperature (T_{cr}) or more accurately right arterial temperature (T_{ra}; which tracks blood temperature bathing

* Corresponding author. Tel.: +1 575 313 4687; fax: +1 575 538 9840.
E-mail address: r2gbiotor@yahoo.com (R.R. Gonzalez).

0306-4565/$ - see front matter © 2010 Elsevier Ltd. All rights reserved.
doi:10.1016/j.jtherbio.2010.09.007

the brain T_{bl}) measured by esophageal temperature at the level of the heart (Sawka et al., 1996, 1988) at 39.5 °C (103 °F) (Wallace et al., 2005; Minard et al., 1957). Heat exhaustion is easily reversible by giving water, cooling, and rest. However, heat stroke, *per se* is a life-threatening situation when it occurs and has been clinically defined with the threshold core temperature (T_{cr})=105.8 °F (41.0 °C) manifested by hot, flushed dry skin, and the presence of central nervous system abnormalities, such as delirium, convulsions, and coma if an afflicted individual is still alive (Gagge and Gonzalez, 1996; Shapiro and Seidman 1990; Wallace et al., 2005; Minard et al., 1957; Glazer, 2005; Jain et al., 2005). Heat stroke has been observed at core temperatures as low as 40.6 °C resulting from an abrupt impairment in homeostatic balance (Kosaka et al., 2004; Broessner et al., 2005). The clinical manifestations resemble acute sepsis (Broessner et al., 2005; Leon et al., 2005) and the critical symptoms present as hypovolemia due to frank dehydration (Kosaka et al., 2004). Heat stroke is diagnosed by an elevated core body temperature (> 40 °C or higher) accompanied by anhidrosis (sweat gland impediments), hot dry skin, and central nervous system abnormalities such as attention deficit, impaired memory, drowsiness, delirium, convulsions, and coma (Epstein et al., 1999; Minard et al., 1957; Glazer, 2005; Jain et al., 2005). The condition is often fatal even if the skin and core body temperatures are adequately reduced because there manifest three important syndromes. These include: an exaggerated acute-phase response, the altered expression of heat-shock protein (HSP) released when cells are exposed to high temperatures, and immune system dysfunction that often lead to inflammatory responses, intravascular coagulation, and multi-organ injury (Leon et al., 2005). The pathologic features of heat stroke, which are similar regardless of the cause of the heat illness, are often shown (but not necessarily evident in an autopsy and can be masked by other systemic failures) by swelling and degeneration of tissue and cell structures, and by widespread, microscopic to massive hemorrhages (Kenney et al., 2004; Jain et al., 2005). Multiple organ dysfunctions occur as the core temperature reaches a critical threshold (Kosaka et al., 2004; Broessner et al., 2005). Most organs are congested, with increased masses and swollen cells. In the gastrointestinal tract, postmortem examination often shows massive ulcerations, hemorrhages, and engorged intestinal vessels. The gut (viscera) is important because: (1) its function determines whether ingested fluid and solutes are delivered to the systemic circulation to correct losses and thereby attenuate hyperthermia, dehydration, and reductions in splanchnic blood flow and gut distress. Furthermore, (2) heat stroke may be exacerbated by gastrointestinal dysfunction, leading to leakage of gut-derived endotoxin (lipopolysaccharide [LPS]) into the circulation, endotoxemia, and consequent circulatory collapse (Shapiro and Seidman, 1990; Kosaka et al., 2004; Glazer, 2005; Leon et al., 2005).

Effective and timely treatment when heat stroke is first diagnosed can reduce the mortality to less than 10–20% (Jain et al., 2005; Leon et al., 2005). Those who survive, however, often have evidence of permanent neurologic impairment and long-term disabilities, especially if the condition is not aggressively and promptly treated (Jain et al., 2005). Rhabdomyolysis (rapid breakdown of skeletal muscle due to injury to muscle tissue) and acute renal failure also may develop even if core and skin body temperatures return to normal levels. In essence, heat stroke is a multisystem physiologic insult that potentially can affect almost every organ system (Shapiro and Seidman, 1990; Glazer, 2005; Jain et al., 2005).

Additionally, the central nervous system (CNS) is especially sensitive to the damaging effects of hyperthermia, CO_2 levels, and pH (Wright and Boulant, 2007). There is generally irreversible damage to the CNS brain cells (Shapiro and Seidman, 1990; Jain et al., 2005). Heat stroke-related long-term CNS sequelae following successful heat stroke treatment include cerebellar deficits, dementia, and personality changes (Shapiro and Seidman, 1990; Glazer, 2005; Cian et al., 2001).

Fig. 1 is a schematic scenario of likely consequences leading to irreversible heat stroke. The figure depicts a rough conception of the consequences that occur when heat stress overwhelms the human physiological system. In general (Gagge and Gonzalez, 1996; Sawka et al., 1996), a normal, healthy human body compensates against temperature rises by increased heat loss occurring via thermal radiation (R), convection (C), conduction (K), and evaporation (E) by sweating and by respiration (E_{res}). In a neutral/comfortable environment, the body does not need to expend excessive thermoregulatory action to preserve its thermal balance. Evaporative heat loss provides some 25% of total heat loss and sensible heat loss (by radiation and conduction) provides some 75% (Gagge and Gonzalez, 1996).

The purpose of this study was to document the critical physiological responses in this heat stroke case study, most likely occurring during the victim's prolonged entrapment, using the best estimate of the environmental stress and validating a thermoregulatory model. The model's output was matched to equivalent environmental observations similar to that of the date of the incident (DOI) (Halford, 2009). In the present case scenario, during the day of the incident (DOI), the preliminary weather

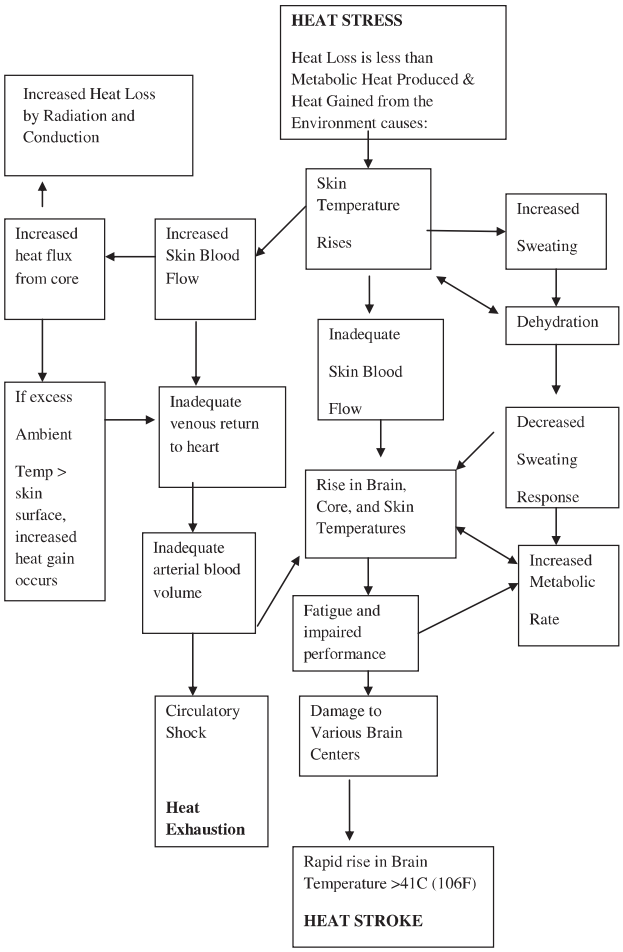

Fig. 1. Schematic representation of a typical cascade of physiologic consequences leading to irreversible heat stroke. See text for details and variables noted.

analyses showed that for the date and time period of the occurrence (1400–1630 h), the outdoor weather had occurred at ambient temperatures between 31.7 and 33.9 °C (89–93 °F). However, such air temperatures did not reveal what were the exact interior temperatures (air and mean radiant temperatures) within the enclosed auto.

The hypothesis is that because of the increased, unabated interior temperature, lack of ventilation, and exterior solar load impinging on the vehicle, a slow, continuous increase in core and skin temperatures and uncompensable physiological parameters resulted in heat storage that led to eventual heat stroke in the individual at the DOI. We hypothesized that a robust, sophisticated, physiological model would reliably document such effects of the heat stroke provocation.

2. Methods

2.1. Environmental study site

We selected a site on the University of Nevada, Las Vegas (UNLV) campus that matched closely the environment of the actual DOI site as far as the parking surface and shading characteristics. This location had the advantage of being fenced off from the public and allowed unhampered conduction of the environmental experiments without having to move and relocate the vehicle. Additionally, the site was located within a few meters of where we measured the corresponding weather data.

We parked the test vehicle in an equivalent heading as the vehicle at the DOI. The azimuth angle of the parking space at the incident site was measured using a Brunton® 8099 sighting compass. The bearing was found to be 95° from north and the test parking space was constructed at this same angle.

2.2. Environmental instrumentation and data acquisition

The exemplar vehicle (and the typical microclimate area around it) was fitted with the following sensors: (1) Four Campbell Scientific® 108-L temperature sensors that tracked the ambient air temperature in the vehicle. The sensors were shielded from solar radiation using a 20.3 cm length of 5.1 cm diameter PVC pipe that was wrapped with reflective tape. We suspended the sensors approximately 30.4 cm above each seat; (2) One Campbell Scientific® 108-L temperature sensor was mounted inside a 15.2 cm diameter matte black copper sphere for measuring the globe temperature (T_g) in the passenger seat; (3) One Campbell Scientific® CS215 temperature and relative humidity sensor (Vaisala) was mounted in the 41303-5a radiation shield suspended at a central location within the car; (4) One Campbell Scientific® CS500-L temperature and relative humidity sensor (Vaisala) was mounted in the 41303-5a radiation shield mounted on a 3.66 m mast located 6.1 m from the car.

Data acquisition was performed using a Campbell Scientific® CR10X datalogger and Am16/32 multiplexer. These instruments were mounted in a protective cabinet and placed behind the vehicle. The leads for the sensors were positioned in the trunk through the hole in the left rear of the vehicle used for the tail light. From the trunk area, the leads were channeled into the vehicle cabin through the collapsible armrest in the rear seat. Such configuration allowed the trunk of the vehicle to be completely closed during the tests, thus avoiding inconsistencies caused by running various sensor leads through a partially open hatch.

The data logger (DA) recorded measurements from all sensors at one-minute intervals and wrote the values to a data file. In addition to the Campbell Scientific System described here, backup measurements were logged using a Questemp QT-36 thermal environment monitor. This is a self-contained DA sensor/data logger that measures and records 5 parameters (dry bulb temperature, natural wet bulb temperature, globe temperature, integrated WBGT, and relative humidity).

2.3. Weather data

Weather data (with the exception of % RH which was measured separately) for the experiment were retrieved each day from the UNLV Measurement and Instrumentation Data Center (MIDC). The parameters measured at the UNLV facility were ambient air temperature (T_a), wind speed (V_a), direct normal solar insolation, and global horizontal solar insolation. The sensors used to make these measurements were situated less than 60 m from the experimental site thus minimizing parameter variations due to location. The station at UNLV is not equipped to measure relative humidity, so these data were provided by the Clark MIDC station. This sensor is located approximately 6.2 km from the experiment site. The instruments used at all MIDC sites are regularly calibrated by the National Renewable Energy Lab (NREL). Details regarding the types of sensors used at each site and the recent calibrations are accessible using the following site: http://www.nrel.gov/midc/

A more extensive record of the environmental parameters recorded and other DA procedures can be found in a report by Halford (2009).

2.4. Environmental data collection and consent procedures

Written informed consent was obtained from the immediate family members responsible for the case study individual and their full approval was given to use any and all data obtained from the heat stroke victim for this simulation. The environmental test procedure was designed to closely match and confirm with the circumstances of the DOI. The heat stroke victim was last seen at 1400 h and was discovered in the car at 1825 h. Data for each test were therefore collected between 1230 and 1830 h. The formal daily test procedure was as follows:

(a) *Each morning of an experimental test evaluation:* Since the vehicle is left parked at the test location, no movement of the vehicle is necessary. Any preliminary inspections that require opening or closing the vehicle doors or trunk were generally completed by 1230 h.
(b) *1230 h:* At this time, the Campbell unit is turned on and the Questemp unit is initiated and placed in the passenger seat. Once this procedure is completed, the vehicle is not disturbed until 1400 h. This 1.5 h period is included in the test to allow the vehicle temperatures to reach steady state and recover from any disturbances or inconsistencies prior to the actual test time. The time period is outside of the time window in which the incident occurred.
(c) *1400 h*: To replicate circumstances by the victim entering the vehicle, the front passenger door was opened fully at exactly 1400 h and left opened for 30 s. A stopwatch was used to measure the time interval. After 30 s, the door was then closed. From this point until the end of the test at 1830 h, there are no further disturbances to the vehicle and the car was left in a "closed" configuration.
(d) *1830 h*: The door was opened to retrieve the Questemp Heat Stress Monitor unit and the data are downloaded into a laptop. The Campbell data are also downloaded at this time.

The weather data for the test are downloaded from the MIDC website when it becomes available the following morning.

Testing was conducted on relatively clear days between 08-25-09 and 09-16-09 for a total of 16 days of data. The raw data were subsequently incorporated into a MS Excel© spreadsheet from which raw data are imported into statistical modeling packages and other model simulation tools.

2.5. Analysis and parameter estimation

Various internal vehicle parameters on the DOI were measured based upon the weather inputs measured for that date day and the data collected during the experiment. The essential parameters tracked over subsequent day were the average internal air temperature (T_{avg}), which is the average of the four air temperature sensors in each of the four seats, the air temperature at the front passenger seat (T_{pass}), the globe temperature (T_g) also at the front passenger seat and the percent relative humidity (%RH), and the derived water vapor pressure (P_a, Torr) in the vehicle.

2.6. Temperature estimates derived from the exemplar auto interior areas

The interior environmental stress in the interior space of the auto was directly affected by a combination of outside ambient air temperature (T_a), minimal air ventilation (V_{avg}), and the intensity of the outside combined solar flux (Sol, W/m^2). The two solar measurements that were recorded throughout the experiments, as direct and global horizontal, were averaged and combined into a single parameter (Sol) that was assumed to fully describe the impact of the thermal stress in the interior space due to effective solar load.

2.7. Thermoregulatory model and validation

For the physiological simulation output, we entered all data collected from the heat stress meter (HSM) monitored by Quest (QuesTemp 36, see Halford, (2009)) that was placed in the passenger seat during all 16 trials. No statistically significant differences ($P>0.05$) were found between the output temperatures from the QuestTemp 36 and the T_g sampled independently by the Campbell environmental data logger used at the UNLV Center for Energy Research site (Halford, 2009).

The deduction was confirmed that the environmental variables tracked at the UNLV site, where the facsimile automobile was stationed, correspond directly with any NIOSH temperature sensors generally used in other heat casualty circumstances (Minard et al., 1957; Adolph, 1938).

Following the extensive environmental analysis, the next task was to simulate probable physiological responses that likely occurred in the victim during the DOI when the victim became trapped in the vehicle during the time period from the first entry through the time until she was found (1825 h). The specific model algorithms used for this study's determination were derived from explicit computer models (Furlong and Gonzalez, 2003; Kraning and Gonzalez, 1997; Gonzalez, 2004; Gonzalez et al., 1997; Pandolf et al., 1986; Reardon et al., 1997) that were developed at the US Army Research Institute of Environmental Medicine, Natick, MA, and are currently being used by the military (Furlong and Gonzalez, 2003; Gonzalez, 2004; Pandolf et al., 1986; Yokota et al., 2010).

Environmental parameters entered into the model's input were T_a, ambient water vapor pressure (P_a, Torr), T_g, and wind speed (V_a, m/s) collected in the interior of the auto. Best approximation clothing insulation (Gonzalez et al., 1997, 2009) was determined from the individual clo values of the garments. Physiologic input variables were the victim's anthropometric characteristics (height, weight, body surface area (BSA), age, gender, metabolic rate, and other variables culled from the coroner's report).

The environmental temperature factors used as input were derived from the best estimate numerical analysis for T_g, T_{avg}, and T_{pass} values determined by analysis of the interior auto microclimate at each time point equivalent on the day of the incident and integrated from the 16 days tested.

Ambient water vapor pressure (P_a, Torr) was derived using Antoine's equation (Gagge and Gonzalez, 1996; Gonzalez et al., 2009) and included as an input variable in the runs and in all parameters of the heat balance equation simulation (HB) in the TR model iterations architecture (Furlong and Gonzalez, 2003; Kraning and Gonzalez, 1997; Gonzalez, 2004) . The key heat loss parameters included: evaporative heat loss (W/m^2), respiratory heat loss (E_{res}) and convective heat loss from the respiratory tract (C_{res}) (both in W/m^2) that were calculated based on the subjects Met level using Fanger's equations (Gagge and Gonzalez, 1996; Gonzalez et al., 2009) as: $E_{res}=0.0023M(42.2-P_a)$ and $C_{res}=0.0014M(35-T_a)$. P_a in the automobile did not rise higher than 10 Torr. Nevertheless, the moisture added by E_{res} and likely attributed to the victim was included in the simulations as was the C_{res} (T_a being greater than the calculated T_{sk} and added to the overall HB).

In the report by Halford (2009), it was shown that every 1 °F change (occurring in the outside ambient dry temperature from a weather station) impacted the T_{avg} of the interior exemplar auto by 0.9 °F. Therefore, in essence, without the inclusion of extensive Solar Load impinging on the auto, interior dry bulb temperature alone within the auto more than likely would not have been excessive to cause the victim to have heat exhaustion/heat stroke during the period of time (4 h) she was trapped in the auto.

From minute to minute data points garnered from the environmental analysis (Halford, 2009), a simple moving average (SMA) for each 10 min interval up to 240 min was determined for the T_g, T_{pass}, and T_{avg} variables. SMA is the unweighted average of the previous n minutes to minute data points recorded. For example, a 10 min simple moving average of each given temperature at a time point becomes the mean of the previous 10 min temperature. If those respective temperatures (T_{avg}, T_g, and T_{pass}, see Fig. 2) values are T_x, T_{x-1},…,T_{x-9}, then the equation is

$$SMA=[T_x+T_{x-1}+\cdots\rangle+T_{x-9}]/10 \quad (1)$$

2.8. Impact of solar load on human responses

Solar radiation constitutes the most important heat load in a standing automobile. This heat load is usually treated differently from the infra-red heat exchange. The complex solar contribution to the total heat load on a person can be expressed as the summed heat absorbed by the skin and clothing (Gagge and Gonzalez, 1996; Adolph, 1938). The direct rays of the sun fall on the projected area of the human as a function of the solar altitude and azimuth. The solar load impinging directly on a person is the product of the person's projected area (in square meters of body surface, m^2) and the intensity of the solar radiation flux (Gagge and Gonzalez, 1996). The skin or clothing reflects a portion of radiation and absorbs the remainder. In the desert with clear skies most of the solar flux is absorbed but sunlight may also influence the person by reflection from the terrain or clouds (albedo effect) (Gonzalez et al., 1997). By far the largest component that

impacted on the car interior heat load of the present case situation in the victim trapped in the automobile was by direct solar radiation (Halford, 2009).

When a first power relation is used to characterize the radiant heat exchange with the environment, the avenues of convection and thermal radiation have much in common. Each avenue depends on the difference between skin and ambient temperature, T_a or mean radiant temperature (MRT), its sequel WBGT (Wallace et al., 2005; Minard et al., 1957; Vernon, 1932), and on a combined heat exchange transfer coefficient (h_c or h_r) (Gagge and Gonzalez, 1996; Minard et al., 1957; Vernon, 1932). Vernon (1932) showed that the mean radiant temperature of the environment could be measured by means of a 6 inch (15.24 cm) globe (T_g), blackened on the outside to simulate the absorptance of a perfect thermodynamic black body. The globe reaches thermal equilibrium (within 20 min) when the heat gain by thermal radiation equals heat loss by convection. The globe temperature (Fig. 2) correlates well with sensation of warmth and provides a direct indication of the impact of sensible heat stress (by R+C). In addition, the globe's size sums the effect of air and radiant temperatures (by solar load) nearly correctly for a standard sized human subject.

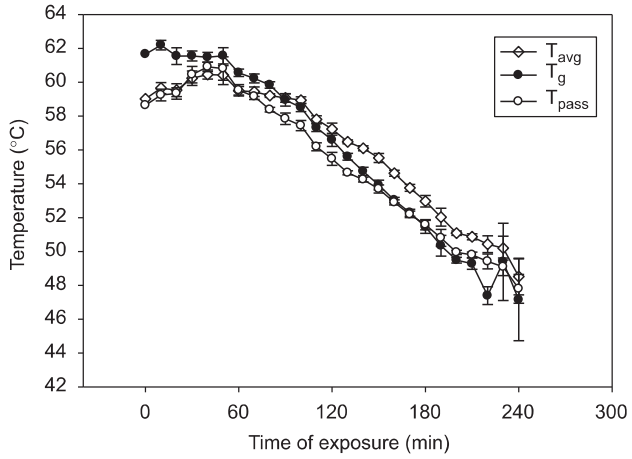

Fig. 2. Time course of temperatures (± 1 SD) recorded in the interior of the facsimile automobile during 16 days of comparable air temperatures to the day of the incident (DOI). Zero time is 1400 h. T_{avg} is the average temperature of 4 sites in the auto, T_g is the 6 inch black globe situated in the passenger side which measures effect of combined solar radiation and mean radiant heat load, and T_{pass} is the temperature of the microclimate in the passenger side where the victim was found. Since the abandoned car had been in the heat for a period of time, T_g is initially elevated at zero time. After 40 min of exposure all temperatures are not statistically different ($P > 0.05$) from each other.

One of the most important applications of the T_g is its use to track the effect of heat stress due to solar load in U.S. Army field operations and its acceptance by the National Institutes of Occupational, Safety, and Health (NIOSH), the US Army, and the US Navy to curb environmental work for military and civilian populations (Sawka et al., 1996; Wallace et al., 2005; Minard et al., 1957; Reardon et al., 1997). The globe is incorporated into the wet bulb globe thermometer (WBGT) index. The index consists of a simple weighting of three temperatures:

$$\text{WBGT}(^\circ\text{F or } ^\circ\text{C}) = 0.7T_{nw} + 0.2T_g + 0.1T_a \quad (2)$$

where T_g is the standard 6 inch black globe, T_a is the shaded dry bulb temperature, and T_{nw} is the unventilated wet bulb (Minard et al., 1957). The most prominent aspect of the index evident in Eq. (2) is that no measurement of air movement is needed (and simulates the situation in the vehicle in the present case). From a health viewpoint, the heat stress conditions depicted by WBGT are those that will cause casualties through heat illness (Wallace et al., 2005).

Table 1
Physiological simulation of heat stroke incidence using environmental input data from a facsimile auto.

Time (min)	T_{ra} (°C)	T_{cr} (°C)	T_{sk} (°C)	T_{mu} (°C)	P_{cas} (%prob)	SR (g/min)	SV (mL)	HR (bpm)	BF_{ra} (L/min)	BF_{cr} (L/min)	BF_{sk} (L/min)	P_{ct}Chg BW%	Likely incidence
0-entry to vehicle	36.8	36.9	36.7	36.2	0.27	4.68	85.6	70	5.95	4.11	1.62	0	
10	36.9	37.1	36.8	36.3	0.28	4.69	84.6	80	6.0	4.21	1.68	−0.15	
20	37.0	37.2	36.9	36.5	0.57	5.63	84.1	78	6.6	3.8	2.6	−0.18	
30	37.1	37.3	36.9	37.1	0.96	6.76	83.5	98	8.3	4.1	3.1	−0.31	
40	37.6	37.7	37.3	37.9	4.11	12.0	85.5	128	10.9	3.1	5.1	−0.51	
50	38.3	38.4	37.9	38.7	32.8	20.5	86.1	141	12.1	2.6	5.8	−0.86	
60	38.8	39.0	38.4	39.3	83.9	25.0	83.6	143	11.9	2.5	5.7	−1.36	
70	39.4	39.5	38.9	39.8	99.0	25.0	81.1	143	11.6	2.5	5.4	−1.88	Heat exhaustion
80	39.8	40.0	39.2	40.3	100	25.0	78.7	143	11.3	2.5	5.0	−2.4	
90	40.1	40.4	39.4	40.7	100	25.0	76.2	144	10.9	2.5	4.7	−2.93	
100	40.4	40.7	39.6	41.0	100	25.0	73.7	145	10.6	2.5	4.3	−3.45	
110	40.6	40.9	39.7	41.2	100	25.0	71.3	145	10.2	2.5	4.0	−3.98	
120	40.8	41.1	39.8	41.4	100	25.0	68.8	145	9.9	2.5	6.6	−4.5	
130	41.0	41.3	39.8	41.6	100	25.0	66.3	145	9.5	2.5	3.3	−5.0**	
140	41.1	41.5	39.8	41.8	100	25.0	63.8	145	9.2	2.5	2.9	−5.6	
150	**41.2**	**41.6**	**39.8**	**41.9**	**100**	**25.0**	**61.3**	**145**	**8.8**	**2.5**	**2.6**	**−6.1**	Heat stroke
160	41.3	41.7	39.7	42.0	100	22.0	58.9	145	8.5	2.5	2.3	−6.6	
170	41.4	41.8	39.6	42.1	100	18.8	56.9	145	8.2	2.5	1.9	−7.0	
180	41.5	41.9	39.5	42.1	100	15.9	55.3	145	7.9	2.5	1.7	−7.4	
190	41.6	41.9	39.4	42.2	100	13.2	53.8	145	7.6	2.5	1.5	−7.7	
200	41.6	42.0	39.2	42.2	100	10.9	52.6	145	7.6	2.5	1.4	−7.9	
210	41.7	42.1	39.1	42.3	100	9.1	51.6	145	7.4	2.5	1.2	−8.1	
220	41.8	42.2	39.2	42.4	100	7.8	50.8	145	7.3	2.5	1.1	−8.3	
230	42.0	42.3	39.5	42.5	100	7.3	49.9	145	7.2	2.5	1.0	−8.5	
240	42.3	42.6	39.8	42.8	100	6.4	49.3	145	7.1	2.5	0.9	−8.6	

Symbols above: T_{ra}=right arterial temperature (bathes brain area); T_{cr}=core temperature; T_{mu}=muscle temperature; T_{sk}=skin temperature; ST=total sweat rate; SV=cardiac stroke volume; HR=heart rate; BF_{ra}=blood flow right atrium; BF_{cr}=blood flow core; BF_{sk}=blood flow skin; P_{ct}ChgBW=% body weight loss without water hydration (** 5% loss).

2.9. Statistical analysis

Statistical analyses were performed using STATISTICA statistical software (Version 8, StatSoft, Inc, Tulsa, OK 74104). Results are presented as means ± SD. Significance was set at $P < 0.05$.

Additional computer modeling code was executed using MS Windows®, Visual BASIC, and Java (Furlong and Gonzalez, 2003; Gonzalez, 2004).

3. Results

3.1. Anthropometry, autopsy report, and blood analysis

Anthropometric body characteristics from the coroner's report were entered as input data variables to derive and validate the physiologic simulation shown in Table 1. These included: body weight (BW)=45.4 kg, height (Ht)=152.4 cm, body fat=14%, age=56 yr, BSA=1.55 m^2, VO_2 at 0.22 L/min, and clothing insulation value (clo value) estimated at 0.2 clo (Gonzalez et al., 1997). The specific somatic form of the individual was classified as Short-Lean, which is used to compare the core temperature simulation necessary to derive a critical heat stroke threshold (Kenney et al., 2004; Wallace et al., 2005; Yokota et al., 2010).

The coroner's report indicated that the prolonged heat stress that the victim was exposed to, more likely than not, resulted in multiple organ failure which led to death. In brief, key post mortem findings included the following: bilateral pulmonary edema, acute renal failure with nephrosclerosis and rhabdomyolysis, and coronary artery hypoplasia quite likely resulting in uncompensable cardiovascular strain and severe progressive dehydration (Sawka et al., 1996; Kenney et al., 2004; Kraning and Gonzalez, 1997; Gonzalez et al., 2009).

Blood analysis was unremarkable and analyses of serum for proinflammatory cytokines were not attainable from which other specific aggravating factors could be determined owing to the heat stroke progression (Kosaka et al., 2004; Leon et al., 2005).

3.2. Environmental analysis

Fig. 2 shows that the interior automobile temperatures were comparable for each time point so the environmental stress governed by each variable was impacting equally on the passenger side of the auto at each time point. We therefore used the T_{pass} and T_g as input variables entered into the model to determine the effect of MRT (i.e., the effective solar load (Gagge and Gonzalez, 1996)) from the summed solar load (Fig. 3). The T_a and T_g were used as inputs in the model (Kraning and Gonzalez, 1997) and the model sequences were iterated over each accumulated 10 min SMA interval up to 240 min. The accumulated heat load (depicted by increase in T_{ra} and T_{cr} shown in Table 1) that the victim experienced is therefore best approximated by this procedure.

The data showed that interior temperatures were between 60 and 63 °C (140–145 °F) from entry to within 80 min; these interior temperatures never fell lower than 46.1 °C (115 °F) for the whole time period of exposure (Fig. 2) with limited ventilation existing in the automobile.

3.3. Thermoregulatory model simulation validation and analysis

Table 1 and Fig. 4 document the simulated physiologic changes that likely occurred during the time of exposure in this case study. The model simulation indicated that a continual increase in the heat stored within the body during the intense heat likely resulted from an impeded ability to dissipate that gained by the environment and her activity level. As blood and core temperature rose and the heat storage increased, the cardiovascular system was placed under increased strain (represented by the cascade in Fig. 1). The irreversible rises in core and skin temperatures are generally associated with increased cognitive performance decrements and disturbed spatial and time orientation (Jain et al., 2005; Cian et al., 2001). All these factors influence the body's ability to deliver blood to the brain and other organs resulting in circulatory shock. Additionally, derived from the model output, Fig. 4A shows that since hydration was not possible, the blood volume is reduced and sweating response is further attenuated exacerbating the increased heart rate and plummeting the cardiac stroke volume so that cardiac output is diminished provocatively (Sawka et al., 1996; Kenney et al., 2004; Epstein et al., 1999; Gonzalez et al., 2009). Such progressive dehydration alters sweat gland function resulting in decreased sweating and reduced skin blood flow and further reductions in plasma volume not replenished by fluid hydration (Sawka et al., 1996, 1988).

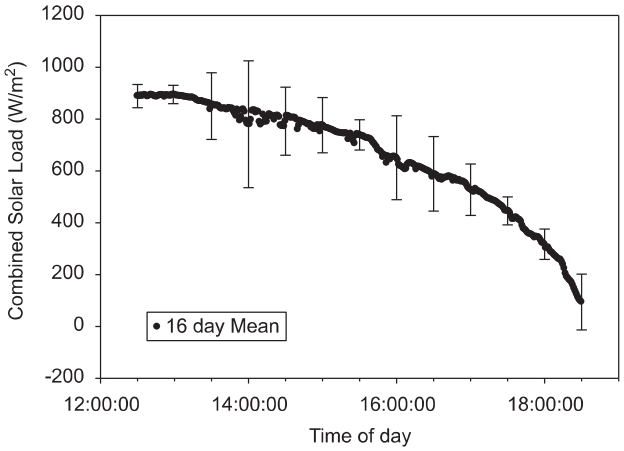

Fig. 3. Combined solar load (W m^{-2}) recorded in the interior of the car. Values are averages (±SD) over 16 days.

The T_{cr} model output at each time point from initial entry into the exemplar vehicle up until the 4 h was matched with equivalent time point WBGT (representing solar heat gain) and T_{pass} values (Figs. 2 and 3, averaged over 16 days). A multiple correlation analysis showed that both β coefficients that compare the relative contribution of each independent variable (WBGT and T_{pass}) were highly significant, $P < 0.001$. Additionally, the proportion of variance accounted for by the correlation between the respective two variables WBGT and T_{pass} versus the dependent variable T_{cr} was 97.9% as expressed by the eigenvalue of 1.96 (Wallace et al., 2005; Yokota et al., 2010).

In addition, the results of the completed environmental analyses on the facsimile auto and a consequent physiological modeling simulation (Table 1) revealed discrete threshold times and probable core temperatures leading to the initial time point of heat exhaustion (core temperatures of 39.5 °C (103.1 °F), a reversible heat stress condition. This was followed by an abrupt rise in T_{cr} to 40.6 °C (105 °F), followed by a gradual rise in T_{cr} to 41.6 °C (106.9 °F) (Table 1).

Comparing our data to a similar meta-analysis study on a healthy military personnel who showed pooled odds ratio (OR) at this cut-off core temperature indicates that at 40.6 °C, individuals are 80–90% at the risk of death (Wallace et al., 2005). From Wallace's (2005) extensive risk-analyses study of military personnel, there is also a high relative risk incidence of fatal

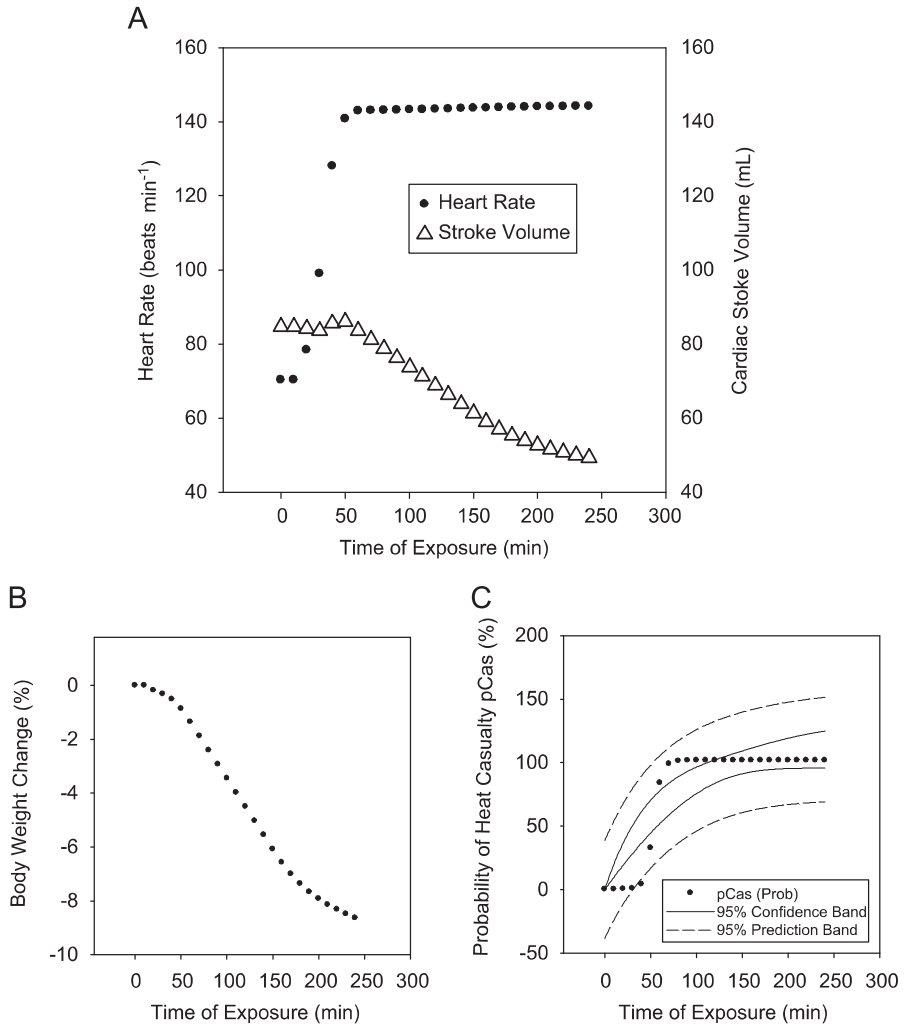

Fig. 4. Physiological model results simulating the day of incident during exposure to heat stress inside a facsimile vehicle. (A) Heart rate and cardiac stroke volume versus time; (B) body weight changes (fluid depletion) versus time; and (C) probability of heat casualty, P_{cas} (%) versus time.

injuries with higher intensity of heat exposures in which WBGT increases $>32\,^{\circ}C$, which confirms the results of the present model output on the heat stroked victim.

Fig. 4C also shows that accompanying the rise in T_{cr} from 39.5 °C at around 80 min, a high probability ($\%P_{cas}$) of heat injury occurs.

4. Discussion

The present heat stress results closely parallel the seminal findings by Adolph (1938) carried out during the Harvard Desert Expedition at Boulder City, NV, in the summer at 1400 h at equivalent air and solar loads of the present case (Fig. 2). Adolph and his associates showed that during resting activities, the solar radiation added heat to the body faster than that heat can be dissipated; pulse rate and systolic arterial pressure increased with rate of heat loss by sweating and skin blood flow and a critical threshold of body weight loss without fluid supplements drastically impaired cognitive performance. The most important finding was that subjects generally were mentally and physiologically impaired by a body weight loss of 2% and loss of consciousness occurred at 5% body weight loss during the intense heat stress.

During heat stress, occurring in prevailing hot weather conditions, the temperature gradient between the skin surface and the environment becomes insufficient to remove the person's metabolic heat. If the body is well hydrated, evaporation of body moisture is a very efficient process that occurs as skin temperature and body core temperature rise. As skin temperature increases, both skin blood flow and sweating increase concomitantly (Fig. 1) and the heat flux from the core body is lost to the ambient. However, when heat balance is threatened by excessive heat gain that is higher than the skin temperature, there is a limited amount of time until excessive thermal discomfort and pain from hot skin dominates. The pain threshold for skin has been shown to be 42 °C (107.6 °F) and generally can only be tolerated no more than 30 sec (Gagge and Gonzalez, 1996). These temperature levels were confirmed by our analysis of the interior seat temperature (Fig. 2) that shows that for the 4.5 h the individual was trapped in the car, the passenger seat temperature dropped no lower than 47 °C (117 °F) (Halford, 2009). For the entire period thermal stress period, the victim's back and upper torso skin temperatures were in contact with the car's interior

temperature that was some 10 °F (5.2 °C) higher than the tolerable pain threshold despite being dressed in light weight clothing (thermal insulation with clo value ≈ 0.2), which offered no protective thermal insulation. The coroner's report showed that 0.645 cm (0.25 inch) pressure marks were evident on the upper back and face of the heat stroked victim confirming this skin–seat contact observation.

Along with the increases in skin temperature and internal body core temperature, the body begins to store the heat that cannot be released by an impeded sweating mechanism. This is an additional intolerable circumstance. Fig. 1 suggests that the increased heat storage sets up an irreversible non-compensatory effect that causes extreme distress and it is only a matter of time until dehydration, inadequate skin blood flow, inadequate arterial blood volume and dangerous rises in core, skin, and brain temperatures. The present study's simulation and validation confirms the increased heat storage. It also shows that this individual experienced this heat storage, undoubtedly, over the whole period of entrapment in the vehicle quite likely leading to the multiple organ failure (Sawka et al., 1996; Kenney et al., 2004).

Current data suggest that the pathophysiological responses to heat stroke may not be due to the immediate effects of heat exposure, per se, but the result of what is referred to as a systemic inflammatory response syndrome (SIRS) that ensues the following thermal injury best studied in a variety of species (Leon et al., 2005). Cytokines are important regulators of the acute phase response to inflammation/injury and have been implicated as mediators of SIRS with heat stroke. There are several lines of evidence supporting a role for cytokines in heat-induced SIRS, including increased circulating levels of cytokines in patients and experimental animals at end-stage heat stroke (Kosaka et al., 2004; Leon et al., 2005).

Heat stroke patients have high values (compared to normal patients with just heat exhaustion) in circulating concentrations of interleukins: IL-1α, IL-1β, IL-1 receptor antagonist, IL-6, IL-10, and tumor necrotic factors (TNF). In some cases, only 30–40% of the patients show increased concentration of a particular cytokine (e.g., IL-1α and IL-10), whereas other cytokines, such as IL-6, are often significantly elevated in 100% of the heat stroke victims (Kosaka et al., 2004; Jain et al., 2005; Broessner et al., 2005; Leon et al., 2005). Unfortunately, post-mortem blood analyses of these important cytokines were not possible in this case study so there is no way to track the extent and confirm blood levels of these variables. Often such blood parameters are not easily obtained and this is why physiological simulation is an important tool in the analysis of heat stress occurrences.

The thermoregulatory model (Furlong and Gonzalez, 2003; Kraning and Gonzalez, 1997; Gonzalez, 2004; Pandolf et al., 1986; Reardon et al., 1997) used in this validation of heat stress analysis has been employed to curb heat stroke fatalities (as a prognostic tool) for similar outdoor environmental heat stress circumstances over the past 15 years. It has been used by the US Army Special Forces, numerous regular troops in Iraq, and NFL football training practices, from 1997 to the present. Our physiological modeling confirmed the classical findings of heat stroke associated with core temperature increases in this victim. The model output showed that with an intense interior car temperature stress and the victim's limited competence, there was, more likely than not, a loss of body mass attributed to fluid loss of 5% at a time point of 130 min. Adolph (1938) similarly showed that his subjects collapsed at such similar fluid loss level. By the time period of 150 min of constant exposure in the car, physiological modeling showed that the victim likely incurred heat stroke conditions with core temperature at 41.6 °C (106.9 °F) and arterial blood (brain) temperatures close to 41.2 °C (106.1 °F).

The selection of threshold points for T_{cr} in Table 1 is based on a well documented meta-analysis of field and laboratory data collected over the past 35 years including a database of over 176,000 healthy U.S. Army recruits with an incidence of 0.6% severe heat illnesses occurring in raw recruits during normal training exercises (Sawka et al., 1996; Wallace et al., 2005). Such evidence suggests that heat illness begins above the point at which heat stress is physiologically compensable, indicating that thermoregulation is effective and a healthy person can still achieve a steady state with a rectal temperature of < 39 °C (102.2 °F) (Sawka et al., 1996; Wallace et al., 2005). However, when thermoregulation is impossible, sweating ceases, and a steady state cannot be reached; then the heat stress is "uncompensable" and heat exhaustion and clinical symptoms of heat stroke can result.

When heat stroke occurs, the body loses any ability to cool sufficiently and essentially all physiologic capacity shuts down. From the data deduced in this case study, it is likely that the heat stroke victim lost consciousness during the DOI at 150 min (Table 1) upon entering the vehicle from this point of time on she was in near death situation. From the modeling data, the time after this point (1.5 hours of additional time of exposure until she was found) only emphasizes the intense brain damage that was likely exhibited during the prolonged heat exposure.

Extensive studies dealing with heat stroke diagnosis, pathophysiological responses, and treatment point out that survival increases if emergency measures are rapidly done ensuring re-normalization of euthermic conditions in the sufferer (Kosaka et al., 2004; Broessner et al., 2005). For the present case study report, theoretically if the victim had been found at a reasonable time and despite current clinical cooling therapies (Casa et al., 2010) employed to minimize tissue injury at the initial onset of heat stroke, it is likely that permanent neurological damage still would dominate. Such brain damage is evident in up to 30% of heat stroke survivors (Jain et al., 2005; Leon et al., 2005). Since the victim was found lifeless by 1830 h (following 240 min of exposure), and CPR was not possible according to all accounts of the incident, it is more likely than not that loss of consciousness and heat stroke conditions evolved at minute 150 to minute 240 resulted in her death.

Our investigation emphasizes that it is critical that a biophysical analysis (such as this one using a reliable TR model) accompany, or should be employed *post hoc* in severe heat stress cases, in addition to early clinical diagnosis that includes internal core temperature measurements in any evaluation of potential heat stroke situations. An important point from the present case study to emphasize evidence of the extreme heat stress experienced by the individual is that the progressive dehydration decreases basal cardiac stroke volume (SV_n) (Fig. 4). There is an almost one for one relationship between the decrement in SV_n and the percentage fall in plasma volume (Sawka et al., 1996, 1988). The severe dehydration leads to cardiovascular strain by impeding cardiac filling pressure, reducing the cardiac stroke volume, and inducing tachycardia (Sawka et al., 1996; Kenney et al., 2004). Consequently, these multiple imbalances translate as important forcing factors that rapidly induce cardiac failure from the heat stroke manifested during extreme environmental heat stress exposure (Table 1 and Fig. 1).

Potentially, a sensor system would be a useful tool in monitoring emergency heat stress conditions and easily integrated with a simple thermoregulatory model algorithm in various microelectronic mechanical systems (MEMS) or even an iPod®. The application of such a tool is especially necessary in monitoring various un-healthy individuals during heat waves. One such circumstance where such a tool is valuable, for example, is during pilgrimages to Mecca, where individuals now conduct their Hajj (many who are aged and un-healthy) in hot seasons [10].

5. Conclusions

Sophisticated and state-of-the art measurements of air temperature, humidity, and solar radiation carried out at the UNLV Center for Energy Research in Las Vegas, which were recorded for 16 days, allowed us to duplicate the weather conditions of the day of the heat stress incident. By this means, we were able to duplicate and ascertain the exact interior heat stress conditions in a facsimile automobile. The *post hoc* environmental data and simulation validations show that

(1) The interior car average temperature (T_{avg}) from a continuous 4-site analysis (passenger, driver, two rear areas) was 59 °C ($\pm$0.32 °C SD) at 1400 h when unwarily the individual entered the vehicle. In the exemplar vehicle, T_{avg} increased to a peak value of 60.4 °C (0.56 °C SD) within 50 min and decreased to a final value at 1830 h of 48.3 °C ($\pm$1.1 °C SD), the time the heat stroke individual was similarly removed from the vehicle.

(2) The combined solar radiation heat stress was assessed on the vehicle's passenger side by two globe temperature measurements, a 6 inch standard globe thermometer (T_g) and a Quest 36 heat stress meter, (displaying WBGT) all currently accepted by NIOSH as suitable measures of heat stress incorporating solar, humidity, and Dry bulb temperature. T_g was 61.7 °C ($\pm$0.3 °C, SD) at 1400 h, remained at this peak level for 60 min and dropped to a value of 49.4 °C ($\pm$0.6 °C, SD) at 1830 h.

(3) The prediction modeling results suggest that from the time of entrapment of the heat stroke victim, simulated core and brain temperatures rose until the time point of heat stroke resulting in multiple organ failure. This threshold point occurred at 2.5 h (150 min). Thus, for the duration of 4.5 h while trapped in the car, the individual was, more likely than not, in a heat stress zone that is considered dangerous by NIOSH and the American College of Sports Medicine.

(4) Our results clearly emphasize that by implementing a human thermoregulatory model (Kraning and Gonzalez, 1997; Gonzalez et al., 1997; Yokota et al., 2010), a tracking of physiological responses of thermal and cardiovascular activity to the heat stress is facile and valuable adjuvant to clinical diagnosis. The U.S. Army and the civilian community have used such models to document physiological changes to heat stress to curb heat stroke in individuals. Results from the present model predictions confirmed that, more likely than not, heat gain from the intense environment and car interior temperatures resulted in inadequate heat balance leading to a cascade of physiological changes (Fig. 1) overwhelming the cardiovascular system and the thermoregulatory system.

(5) This cascade of events began definitely by a rise in brain, core, and skin temperatures, overall fatigue, and impaired ability, and potentially caused irreversible damage to brain centers and uncompensable heat stroke.

Acknowledgments

The authors appreciate the constructive comments of Mr. Rob Murdock and the assistance of Professor Robert Boehm, Director, Energy Research Center, University of Nevada, Las Vegas, during completion of this study. We thank specific family members for allowing us the access to essential medical information and data from the present case study's heat stroke victim.

References

Adolph, E.R., 1938. Heat exchanges of man in the desert. Am. J. Physiol 123, 486–499.
Boulant, J.A., 1996. Hypothalamic neurons regulating body temperature. In: Fregly, M.J., Blatteis, C.M. (Eds.), Handbook on Adaptation to the Environment. Part I, The Thermal Environment. American Physiological Society, Rockville, MD, pp. 105–126.
Boulant, J.A., Gonzalez, R.R., 1977. The effect of skin temperature on the hypothalamic control of heat loss and heat production. Brain Res 120, 367–372.
Broessner, G., Beer, R., Franz, G., Lackner, P., Engelhardt, K., Brenneis, C., Pfausler, B., Schmutzhard, E., 2005. Case report: severe heat stroke with multiple organ dysfunction—a novel intravascular treatment approach. Critical Care 9, R498–R501.
Casa, D.J., Kenny, G.P., Taylor, N.A.S., 2010. Immersion treatment for exertional hyperthermia: cold or temperate water? Med. Sci. Sports Exerc. 42 1246–1252.
Cian, C., Barraud, P.A., Melin, B., Raphel, C., 2001. Effects of fluid ingestion on cognitive function after heat stress or exercise-induced dehydration. Int. J. Psychophysiol. 42, 243–251.
Epstein, Y., Moran, D.S., Shapiro, Y., Sohar, E., Shemer, J., 1999. Exertional heat stroke—a case series. Med. Sci. Sports Exerc. 31, 224–228.
Furlong, J.R., Gonzalez, R.R., 2003. Enhancement and integration of thermal strain modeling tools to support objective force warrior: SCENARIO-J v1.0 and SCENARIO-MC v 6.0 DAMD17-98-d0022, Science Applications International Corporation (SAIC), McLean, VA.
Gagge, A.P., Gonzalez, R.R., 1996. Mechanisms of heat exchange: biophysics and physiology. In: Fregly, M.J., Blatteis, C.M. (Eds.), Handbook on Adaptation to the Environment. Part I, The Thermal Environment. American Physiological Society, Rockville, MD, pp. 45–84.
Garigan, T., Ristedt, D.E., 1999. Death from hyponatremia as a result of acute water intoxication in an Army Basic Trainee. Mil. Med. 164, 234–237.
Glazer, J.I., 2005. Management of heat stroke and heat exhaustion. Am. Fam. Physician 71, 2133–2140.
Gonzalez, R.R., 2004. SCENARIO revisited: comparisons of operational and rational models in predicting human responses to the environment. J. Therm. Biol. 29, 515–527.
Gonzalez, R.R., McLellan, T.M., Withey, W.R, Chang, SK., Pandolf, K.B., 1997. Heat strain models applicable for protective clothing systems: comparison of core temperature response. J. Appl. Physiol. 83 (1997), 1017–1023.
Gonzalez, R.R., Cheuvront, S.N., Mountain, S.J., Goodman, D.A., Blanchard, L.A., Berglund, L.G., Sawka, M.N., 2009. Expanded prediction equations of human sweat loss and water needs. J. Appl. Physiol. 107, 379–388.
Halford, C., 2009. An experimental study of internal vehicle temperatures for a 1989 BMW 535i in Las Vegas, NV. UNLV Center for Energy Research Report..
Jain, R., Sawhney, S., Hussein, S., Koul, R., 2005. Neurological damage in heat stroke in a child: CT, MRI, and SPECT appearances. The Internet J. Radiol. 4, 1–12.
Kenney, W.L., DeGroot, D.W., Holowatz, L.A., 2004. Extremes of heat tolerance: life at the precipice of thermoregulatory failure. J. Therm. Biol. 29, 479–485.
Kosaka, M., Yamane, M., Ogai, R., Kato, T., Ohnishi, N., Simon, E., 2004. Human body temperature regulation in extremely stressful environment: epidemiology and pathophysiology of heat stroke. J. Therm. Biol. 29, 495–501.
Kraning, K.K., Gonzalez, R.R., 1997. A mechanistic computer simulation of human work in heat that accounts for physical and physiological effects of clothing, aerobic fitness, and progressive dehydration. J. Therm. Biol. 22, 331–342.
Leon, L.R., Blaha, M.D., DuBose, D.A., 2005. Time course of cytokine, corticosterone, and tissue injury responses in mice during heat strain recovery. J. Appl. Physiol. 100, 1400–1409.
Minard, D., Belding, H.S., Kingston, J.R., 1957. Prevention of heat casualties. J. Am. Med. Assoc 165, 1813–1818.
Pandolf, K.B., Stroschein, L.L., Drolet, L., Gonzalez, R.R., Sawka, M.N., 1986. Prediction modeling of physiological responses and human performance in the heat. Comput. Biol. Med. 6 (1986), 319–329.
Reardon, M.J., Gonzalez, R.R., Pandolf, K.B., 1997. Applications of predictive environmental strain models. Mil. Med. 162, 136–140.
Sawka, M.N., Gonzalez, R.R., Young, A.J., Muza, S.R., Pandolf, K.B., Latzka, W.A., Dennis, R.C., Valeri, C.R., 1988. Polycythemia and hydration: effects on thermoregulation and blood volume during exercise-heat stress. Am. J. Physiol. 255 (1988), R456–63.
Sawka, M.N., Wenger, C.B., Pandolf, K.B., 1996. Thermoregulatory responses to acute exercise-heat stress acclimationIn: Fregly, M.J., Blatteis, C.M. (Eds.), Handbook on Adaptation to the Environment. Part I, The Thermal Environment. American Physiological Society, Rockville, MD, pp. 157–185.
Shapiro, Y., Seidman, D.S., 1990. Field and clinical observations of exertional heat stroke patients. Med. Sci. Sports Exerc. 22, 29–35.
Vernon, H.M, 1932. The measurement of radiant heat in relation to human comfort. J. Ind. Hyg. Toxicol 14, 95–111.
Wallace, R.F., Kriebel, D., Punnett, L., Wegman, D.H., Wenger, C.B., Gardner, J.W., Gonzalez, R.R, 2005. The effects of continuous hot weather training on risk of exertional heat illness. Med. Sci. Sports Exerc. 37, 84–90.
Wright, C.I., Boulant, J.A., 2007. Carbon dioxide and pH effects on temperature sensitive and -insensitive hypothalamic neurons. J. Appl. Physiol. 102, 1337–1366.
Yokota, M, Berglund, L.G., Bathalon, G.P., Monte, G.P., 2010. Carlo simulations of individual variability and their effects on simulated heat stress using thermoregulatory modeling. J. Therm. Biol 35, 154–159.